Reaction Kinetics of Multiphase Polymer Systems under Flow

Lian-Fang Feng
State Key Laboratory of Polymer Reaction Engineering, College of Materials Science and Chemical Engineering,
Zhejiang University, Hangzhou, China

Laboratory of Chemical Engineering Sciences, CNRS-ENSIC-INPL, Nancy, France

Guo-Hua Hu
Laboratory of Chemical Engineering Sciences, CNRS-ENSIC-INPL, BP 451, 54001 Nancy, France

DOI 10.1002/aic.10253

For given nominal molar concentrations in complementary functional groups, the common wisdom is that the reaction rate of those attached to large molecules does not exceed that of small molecule analogues. They are at best equal. The difference in reaction kinetics is more pronounced if reactive molecules are so large that they phase-separate, which is often so for polymers. In such cases, complementary functional groups from the two phases can meet and react only at the interfaces. Thus, reaction kinetics of functional groups attached to small molecules has always been taken as the upper bound for those attached to polymers. Here we show that under sufficient mixing, reaction kinetics of two immiscible reactive polymers can be significantly higher than that of small molecule analogues. This phenomenon is attributed to the combined effects of increasing collision probability originated from mixing-induced interfacial area generation, longer relaxation time of reactive polymer chains, and eventually interfacial slip.
© 2004 American Institute of Chemical Engineers *AIChE J,* 50: 2604–2612, 2004
Keywords: polymer blends, interfaces, flow, mixing, kinetics

Introduction

Chemical reactions between functional groups have found numerous applications in many fields, such as organic synthesis, step polymerization (Odian, 1981), and reactive polymer blending (Baker et al., 2001). To the best of the authors' knowledge, there are no experimental and theoretical studies reporting that, for given nominal molar concentrations in complementary functional groups, the reaction rate of those attached to polymer chains can eventually exceed that of small molecule analogues. In other words, the reaction rate of functional groups attached to small molecules has always been taken as the upper bound of those attached to polymers. They are at best equal. This is possible if reacting systems are homogeneous at a molecular level and the intrinsic reactivity of the functional groups is independent of molecular size. For example, Bhide and Sudborough (1925) studied the kinetics of the esterification of a series of homologous carboxylic acids of type $H(CH_2)_xCO_2H$ with ethanol

$$H(CH_2)_xCO_2H + C_2H_5OH \xrightarrow{HCl} H(CH_2)_xCO_2C_2H_5 + H_2O$$

Those homologous carboxylic acids differed only in molecular size. The latter was characterized by the number of the CH_2 repeating unit, x, in the molecule. They found that, although there was a decrease in reactivity with increased molecular

---

Correspondence concerning this article should be addressed to G.-H. Hu at hu@ensic.inpl-nancy.fr.

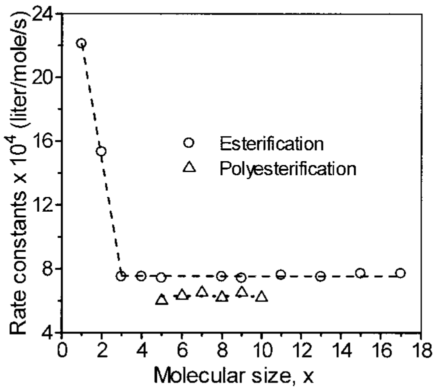

Figure 1. (○) Rate constants for the esterification of a series of homologous carboxylic acids of type $H(CH_2)_xCO_2H$ with ethanol at 25°C.

Note that the rate constant reaches a limiting value and remains constant for $x = 3$; (△) Rate constants for the polyesterification of sebacoyl chloride with a series of homologous α,ω-alkane diols of type $HO(CH_2)_xOH$ at 26.9°C. Note that the rate constant is the same for $5 \leq x \leq 10$.

size, the effect was significant only at a very small size. The reaction rate constant very quickly (at $x = 3$) reached a limiting value, which remained constant and independent of molecular size (Figure 1). Analogous results were found for the polyesterification of sebacoyl chloride with a series of homologous α,ω-alkane diols of type $HO(CH_2)_xOH$ (Ueberreiter and Engel, 1977)

$$HO(CH_2)_xOH + ClOC(CH_2)_8COCl \rightarrow H\!\left[O(CH_2)_xOCO(CH_2)_8CO\right]_n Cl + HCl$$

There are two scenarios where the reaction rate constant may no longer remain constant but decrease significantly with increased molecule size. First, the reactivity of the functional groups is so high and/or the polymer is so large that the bulk diffusion of the polymer chains becomes the limiting step of the reaction rate. Second, polymers to which complementary functional groups are attached are immiscible at a chain level and their mixture phase-separates. This is often the case for two dissimilar polymers because of the very small entropy of mixing compared to that of small molecule analogues. In such a phase-separated polymer reacting system, complementary functional groups from the two phases can meet and react only in the interfacial regions (Fredrickson, 1996; O'Shaughnessy and Sawhney, 1996). Thus, only small fractions of them have opportunities to collide and react and most of them are excluded from such opportunities.

Here we show experimentally that if polymer chains to which complementary functional groups are attached are immiscible and mixing to which the system is subjected is strong enough, the reaction kinetics can be significantly faster than that of small molecule analogues. For that purpose, we could envision comparing the kinetics of four reactive systems, all containing the same numbers of A and B functional groups (see Figure 2). In system (a), molecules bearing A and B functional groups are small and mutually miscible. System (b) differs from system (a) only in that the B functional group is attached to a polymer. Nevertheless, they remain miscible. In system (c), both A and B functional groups are attached to a polymer of the same chemical nature. The system is thus miscible. In system (d), A and B functional groups are attached to polymers of different chemical natures, which are immiscible. In other words, in the first three homogeneous systems, the A and B functional groups are randomly distributed over the entire reaction volume at the scale of their size. In the last heterogeneous system, given that A-bearing polymer and B-bearing polymer are immiscible, most of the A and B functional groups are located in their respective polymer phases. Only small fractions of them are located in the interfaces between the two polymer bulk phases. The interfaces are the only locations where they can collide and react. If the nominal molar concentrations of the reacting functional groups in the above four reactive systems are equivalent, the common wisdom regarding their reaction rates follows the order: (a) ≥ (b) ≥ (c) ≫ (d). In this study, we choose systems (b) and (d) to show that for given nominal molar concentrations in A and B functional groups, contrary to the above common wisdom, *undermixing* the reaction rate of system (d) can eventually exceed that of system (b). We then attempt to explain why and how this is possible.

Experimental

Materials

A heterogeneous reacting system and a homogeneous one were chosen for this study. They were based on the well-known reaction between hydroxyl and isocyanate groups. The nominal molar concentrations of those two complementary functional groups in both reacting systems were the same. Moreover, the molar ratio between the hydroxyl and isocyanate groups was unity. The heterogeneous reacting system corresponded to system (d) in Figure 2. It was composed of a chemically inert polystyrene (PS); a PS end-functionalized with a hydroxyl

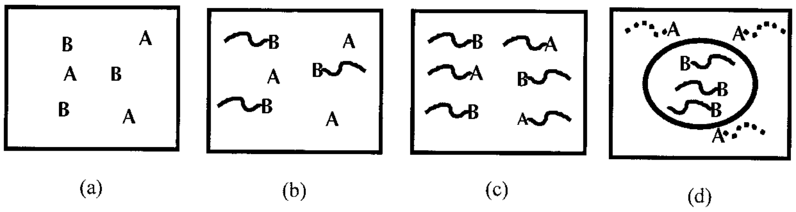

(a) (b) (c) (d)

Figure 2. Four reacting systems could be envisioned for this study.

(a) Miscible system of A + B; (b) miscible system of A + B–bearing polymer; (c) miscible system of A-bearing polymer + B-bearing polymer; (d) immiscible system of A-bearing polymer + B-bearing polymer. Note that all four reacting systems contain equivalent numbers of A and B functional groups.

group, denoted as PS–$(CH_2)_2$–OH; a chemically inert poly(methyl methacrylate) (PMMA); and an isocyanate-bearing PMMA, denoted as PMMA-*r*-NCO. The PS–$(CH_2)_2$–OH was synthesized anionically and the PMMA-*r*-NCO by free-radical copolymerization of MMA with 3–3-isopropenyl-α,α-dimethylbenzyl isocyanate (Hu and Kadri, 1998, 1999). The content of the isocyanate-bearing monomer incorporated into the PMMA-*r*-NCO was 1.5 wt %, which corresponded, on average, to 2 NCO moieties per PMMA-*r*-NCO chain. The number molar mass of the PS, PS–$(CH_2)_2$–OH, PMMA, and PMMA-*r*-NCO was 175, 53.7, 50.0, and 27.9 kg/mol, respectively. Their polydispersity indices were 2.28, 1.05, 2.20, and 3.24, respectively. The above PS/PMMA heterogeneous reacting system was studied using five different mass compositions: 72/25, 60/40, 50/50, 40/60, and 25/75. The mass composition of the PS–$(CH_2)_2$–OH and that of the PMMA-*r*-NCO therein were always kept unchanged, that is, 12 and 2.4 wt % with respect to the total reacting mass, respectively. The homogenous analogous reacting system corresponded to system (b) in Figure 2. It was composed of the PMMA, the PMMA-*r*-NCO, and 3-phenyl 1-propanol. The latter was analogous to PS–$(CH_2)_2$–OH and will be denoted as Ph–$(CH_2)_3$–OH. Both reacting systems were catalyzed by dibutyl tin dilaurate (50 ppm with respect to the total reaction mass). The reason for using the said catalyst was that without a catalyst, the kinetics of the above two reacting systems were so low that it was difficult to detect conversions attained within the experimental timescale, of the order of 1 h (a much longer reaction time would bring about side reactions). In fact, a separate study (Li, 2000) showed that the reaction rate of the above homogeneous reacting system without catalyst was an order of magnitude lower than that with 50 ppm of the said catalyst. Moreover, the said catalyst was found to be soluble in PS and PMMA within the concentration range used. Thus, it was likely that the catalyst was evenly distributed in the entire PS/PMMA heterogeneous reacting system including the interfacial regions. Thus, it was likely that the catalyst was evenly distributed in the entire PS/PMMA heterogeneous reacting system including the interfacial regions.

Reaction and characterization procedures

An internal Haake-type batch mixer (Haake, Bersdorff, Germany) was used to carry out the reactions of the above two reacting systems. It was composed of a figure 8–shaped chamber. Mixing of the reacting systems was ensured by the rotation of two rotors in the chamber. The temperature of the reaction was set at 175°C. Samples were taken from the chamber at chosen time intervals for subsequent analyses. The extent of reaction was determined with respect to the conversion of the NCO group. The latter was measured by a two-step method. The first step was to react the remaining NCO moieties in the PMMA-*r*-NCO with 9-(methylamino-methyl)anthracene in a quantitative manner. In the second step, the amount of the anthracene moieties attached onto the PMMA-*r*-NCO was measured by ultraviolet spectroscopy. That method was able to measure NCO moieties in the level of a few ppm (Hu and Kadri, 1998, 1999; Hu et al., 1999). Its validity was also confirmed by infrared spectroscopy (IR), which used the absorbance of the peak at 2255 cm^{-1} to quantify the amount of the NCO. However, the IR method worked well only when the amount of the remaining NCO was high enough (Li, 2000). The morphology of blends was characterized by transmission electron microscopy (TEM) using films about 50 nm thick. Before analysis, the films were stained for 2 h with the vapor of 0.5% OsO_4 in water solution. The PS phase was preferably stained and appeared dark in TEM micrographs.

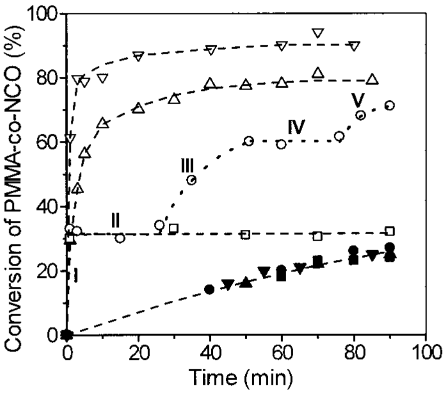

Figure 3. Time dependency of the conversion for the Ph–$(CH_2)_3$–OH/(PMMA + PMMA-*r*-NCO) homogeneous small molecule alcohol reacting system (closed symbols) and the [(PS + PS–$(CH_2)_2$–OH]/(PMMA + PMMA-*r*-NCO) (60/40) heterogeneous macromolecular alcohol reacting system (open symbols) under three mixing conditions.

(▽, ▼): continuous mixing at 84 rpm; (△, ▲): continuous mixing at 64 rpm; (□, ■): stepwise mixing with the rotation speed alternating between 0 at 64 rpm; (○, ●): without mixing, except for the very first minute during which the rotation speed was 64 rpm to ensure melting and a certain degree of homogenization of both reacting systems.

Results

Figure 3 shows the conversion as a function of time of the Ph–$(CH_2)_3$–OH/(PMMA + PMMA-*r*-NCO) homogeneous small alcohol system (closed symbols) and the [PS + PS–$(CH_2)_2$–OH]/(PMMA + PMMA-*r*-NCO) (60/40) heterogeneous macromolecular alcohol system (open symbols) under one of the three following mixing conditions: (a) continuous mixing at 64 or 84 rpm (rpm) for the entire reaction time; (b) stepwise mixing with the rotation speed alternating between 0 at 64 rpm; (c) without mixing, except for the very first minute, during which the rotation speed was 64 rpm to ensure melting and a certain degree of homogenization of the reacting systems. In the case of the homogeneous small alcohol reacting system, mixing had little effect on the reaction rate because the conversion followed the same pace, regardless of the mixing condition. This implies that, in that homogeneous system, the bulk diffusion of the reactive molecules was most likely not the rate-limiting step of the reaction rate. By contrast, the reaction rate of the heterogeneous macromolecular alcohol system depended very strongly on the mixing condition. The stronger the mixing, the higher the reaction rate. The conversion increased more rapidly at 84 rpm than at 64 rpm, especially in the very early stage of mixing. Without mixing (the rotation speed being zero), the reaction rate became zero. This was further corroborated by the experiment carried out under the stepwise mixing

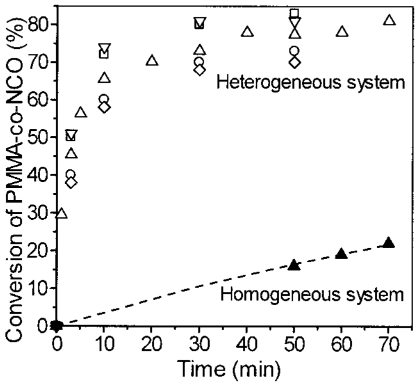

Figure 4. Effect of composition on the rate of conversion increase of the [PS + PS–$(CH_2)_2$–OH]/(PMMA + PMMA-*r*-NCO) heterogeneous macromolecular alcohol reacting system.

(○) 72/25, (△) 40/60, (□) 50/50, (▽) 60/40, (◇) 25/70. The corresponding data of the Ph–$(CH_2)_3$–OH/(PMMA + PMMA-*r*-NCO) homogeneous small molecule alcohol reacting system are also shown for comparison (▲). Mixing condition: continuous mixing at 64 rpm.

condition. In stage I (0 to 1 min), in which the mixing speed was 64 rpm, the conversion increased very rapidly. In stage II, mixing was stopped and the reaction stopped proceeding. Once mixing was resumed, the reaction started to proceed again (stage III). It stopped again in stage IV where there was no mixing. It quickly started to proceed again under mixing (stage V). These results show that the reaction rate of the heterogeneous macromolecular alcohol system was controlled by the rate of mixing or the rate of interfacial area generation. Comparison of the kinetic data shows that under the specified continuous mixing conditions, although both the heterogeneous and homogeneous reacting systems contained equivalent nominal concentrations in the hydroxyl and isocyanate groups, the overall reaction rate (defined as the slope of a conversion–time curve) of the heterogeneous one was much faster than that of the homogeneous one, at least in the first 5–10 min of the reaction. Because those mixing conditions are commonly met in practical reactive polymer-blending processes, it is expected that on the basis of equal molar concentrations in reacting functional groups, the reaction rates of immiscible reactive polymer systems can be higher than those of small molecule analogues.

Figure 4 compares the rate of reaction of the PS/PMMA heterogeneous reacting system of five different mass compositions in PS and PMMA: 75/25, 60/40, 50/50, 40/60, and 25/75. Recall that the amounts of the reactive polymers involved in all those five compositions were the same. Clearly, the composition had an effect on the rate of the conversion increase and on the ultimate conversion value. They were highest at 50/50 and 60/40 and lowest at 75/25 and 25/75. This may be explained by the fact that at 50/50 and 60/40, the morphology of the system was of co-continuous type, exhibiting highest interfacial areas. At 75/25 and 25/75, it was of dispersion type, whose interfacial areas were smallest. Nevertheless, whatever the composition, the reaction rate of the PS/PMMA heterogeneous reacting system was always significantly higher than that of its homogeneous analogue.

Discussion

The two complementary functional groups involved in the homogeneous small molecule alcohol reacting system are distributed randomly at the scale of their size over the entire volume of the reacting system (Figure 2b). The reaction between them is a product of their random collisions occurring over the entire reaction space. The fact that the reaction rate of the homogenous small alcohol reacting system is not mixing-controlled implies that mixing most likely did not alter the random distribution feature of the functional groups nor their collision mode and frequency. The latter refers to the number of collisions per unit time. By contrast, the two complementary functional groups involved in the heterogeneous macromolecular alcohol reacting system are no longer distributed randomly at the scale of their size over the entire volume of the reacting system. Instead, they are highly segregated (Figure 2d). The hydroxyl and isocyanate groups are located primarily in the PS and PMMA bulk phases, respectively. The interfacial regions between both phases are the only locations where the two complementary functional groups can meet, collide, and react. This is demonstrated unambiguously by the kinetic results shown in Figure 3. The fact that the rate of reaction is entirely controlled by the rate of mixing implies that the collision frequency of the functional groups increases with increasing mixing rate.

How does mixing increase the collision frequency of the complementary functional groups in the heterogeneous macromolecular alcohol reacting system? Mixing is expected to play two positive roles in promoting collision of functional groups in an immiscible reactive polymer blend. The very first, obvious, and probably the most important one is to increase the interfacial area (Guegan et al., 1994). This is shown by the two TEM micrographs in Figure 5. Micrographs (a) and (b) correspond to the [PS + PS–$(CH_2)_2$–OH]/(PMMA + PMMA-*r*-NCO) (60/40) heterogeneous macromolecular alcohol reacting system after 1 and 40 min of mixing at 84 rpm, respectively. The amount of the total area of the interfaces between the PS and PMMA phases, generated after 40 min of mixing, is greater than that generated after 1 min of mixing. Correspondingly, the size of the PMMA dispersed phase domains after 40 min of mixing is smaller than that after 1 min of mixing. In what follows, specific interfacial area will be used to quantify the amount of the interfacial area. It is defined as the amount of the interfacial area per unit volume of the dispersed phase. Figure 6 shows the evolution of the specific interfacial area in $\mu m^2/\mu m^3$ and the volume-average diameter of the PMMA domains (in μm) as a function of mixing time for the heterogeneous macromolecular alcohol reacting system at two mixing speeds: 64 and 84 rpm. Under both mixing speeds, the specific interfacial area first increased very rapidly and then leveled off. Correspondingly, the volume-average diameter of the PMMA domains first decreased very rapidly and then reached a limiting value, which remained constant. The lower the mixing speed, the longer time it took to reach the limiting values of the specific interfacial area and the volume-average diameter, as expected. An increase in interfacial area increased the number of contacts and collisions between the two complementary reacting functional groups.

The second effect of mixing is to accelerate the process of copolymer pull-out from the interfaces (Charoensirisomboon el

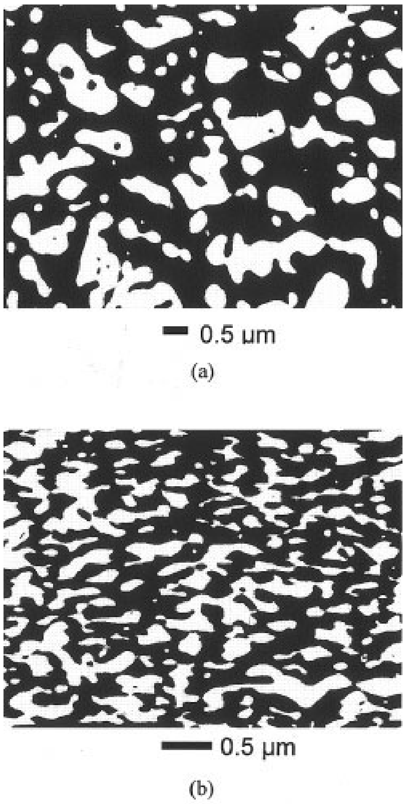

Figure 5. TEM micrograph of the [PS + PS–$(CH_2)_2$–OH]/(PMMA + PMMA-*r*-NCO) (60/40) heterogeneous reactive blend after 1 and 40 min of mixing, respectively.

The mixing speed was 84 rpm.

al., 2000; Lyu et al., 1999), generating additional fresh interfaces free of copolymer coverage. This mixing process may be called interfacial mixing. A copolymer chain formed in situ at an interface may leave the interface for thermodynamic and/or hydrodynamic reasons. The degree to which copolymer chains can be pulled out from the interfaces by mixing depends, among other factors, on their architecture, the areal density of copolymer chains at the interfaces, and mixing condition. According to Charoensirisomboon et al. (2000), for a given molar mass, a block copolymer with linear chain structure is more easily pulled out than a graft copolymer with branch structure. An inversed Y-shaped graft copolymer with the trunk chain located in the dispersed phase and the branch in the matrix is much less prone to mixing-induced pull-out than a Y-shaped graft copolymer with the trunk chain located in the matrix and the branch in the dispersed phase.

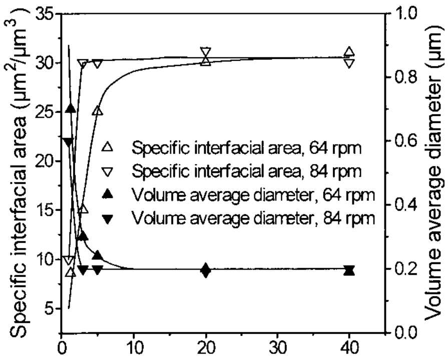

Figure 6. Time dependency of the evolution of the morphology of the [PS + PS–$(CH_2)_2$–OH]/(PMMA + PMMA-*r*-NCO) (60/40) heterogeneous reacting system in terms of the specific interfacial area (open symbols) and the volume-average diameter (closed symbols).

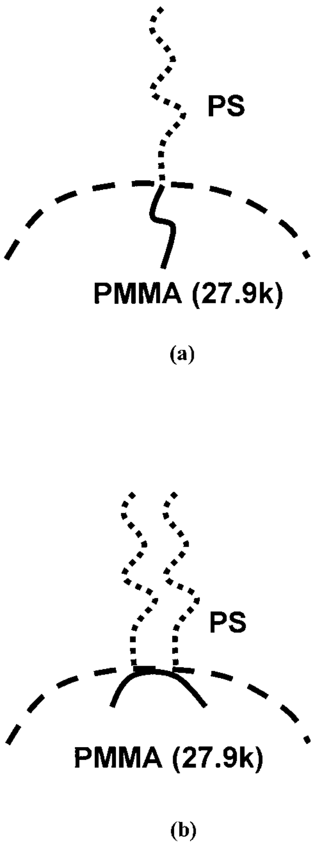

Figure 7. Schematic representation of the architecture of the in situ formed graft copolymers in the [PS + PS–$(CH_2)_2$–OH[/(PMMA + PMMA-*r*-NCO) (60/40) immiscible reactive blend.

Numbers in the brackets are the number-average molar mass of the reactive component polymers: (a) an inversed Y-shaped graft copolymer when one of the two NCO moieties of the PMMA-*r*-NCO is reacted; (b) an inversed Π-shaped graft copolymer when both NCO moieties of the PMMA-*r*-NCO are reacted. The numbers in the brackets are the number-average molar masses of the PMMA trunk chain and a single PS branch.

Recall that the PMMA-*r*-NCO chain contained, on average, 2 NCO moieties per chain and the PMMA phase was the dispersed phase of the reactive blending system under study. If one of the two NCO moieties of a PMMA-*r*-NCO chain was reacted, an inversed Y-shaped PMMA-*g*-PS graft copolymer with one PS graft was formed (see Figure 7) and its number-average molar mass was 81.6 kg/mol. If both NCO moieties were reacted, an inversed Π-shaped graft copolymer with two PS grafts was formed and its number-average molar mass was

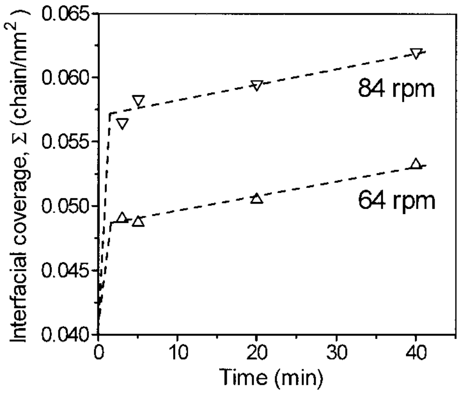

Figure 8. Time dependency of the interfacial coverage Σ by the in situ formed graft copolymer in the [PS + PS–$(CH_2)_2$–OH]/(PMMA + PMMA-*r*-NCO) (60/40) reactive blend.

(▽), 84 rpm; (△), 64 rpm.

then 109.5 kg/mol. For both graft copolymers, the PMMA was the trunk chain having a number-average molar mass of 27.9 kg/mol and was preferably located in the PMMA dispersed phase. The PS was the branch(es), with each having a number-average molar mass of 53.7 kg/mol. It was preferably located in the PS matrix phase. How stable were those two graft copolymers formed in situ at the interfaces between the PS and PMMA phases undermixing? Were they pulled out of the interfaces by mixing? If they were, they would either form micelles of 10 to 20 nm in size or be dissolved in the PS matrix at the scale of chain dimension. If micelles were formed, they could be detected by TEM. None of the TEM micrographs of the PS/PMMA reactive blend revealed the existence of such micelles, including the one corresponding to 40 min of mixing at 84 rpm (see Figure 4b). This implies that the in situ graft copolymers likely did not form micelles in the PS matrix. Were they then dissolved therein? This could be possible considering the relatively low interaction parameter between PS and PMMA, $\chi_{\text{PS–PMMA}} = 0.0129 + 1.96/T$ and 0.017 at 175°C (Mark, 1996). However, TEM can hardly detect dissolved graft copolymers. Nevertheless, it should be kept in mind that the in situ–formed graft copolymer was either an inversed Y-shaped graft copolymer or an inversed Π-shaped graft copolymer. According to Charoensirisomboon et al. (2000), this type of graft copolymer is difficult to be pulled off the interfaces. On the other hand, the asymmetry in length between the PMMA trunk and the PS graft favors the copolymer pull-out.

Let us evaluate the areal density of the in situ–formed graft copolymer chains at the interfaces, Σ, which is defined as the number of their chains per unit interfacial area. Figure 8) shows the time dependency of the interfacial coverage Σ by the in situ–formed graft copolymer in the [PS + PS–$(CH_2)_2$–OH]/(PMMA + PMMA-*r*-NCO) (60/40) immiscible reactive blend (see Appendix for the procedures used to estimate Σ). The interfacial coverage increased very rapidly in the very early stage of mixing and quickly slowed down. Moreover, the value of the interfacial coverage was higher at a higher mixing speed. It should be noted that the highest value of the interfacial coverage in Figure 8 is still lower than the maximum interfacial coverage, Σ_{max}, which is estimated to be 0.085 (see Appendix for the procedures used to estimate Σ_{max}).

It is straightforward to understand that mixing promotes the overall reaction rate between two immiscible reactive polymers by generating interfacial area and/or eventually by accelerating the copolymer pull-out process. The latter in turn creates additional interfacial area. However, these two mixing-induced interfacial area generation mechanisms do not seem to be enough to explain our finding that *undermixing* and with equivalent nominal molar concentrations in functional groups, the reaction rate of the heterogeneous macromolecular alcohol reacting system was significantly faster than that of the homogenous small alcohol analogue. This is because, under the specified conditions, the two immiscible reacting polymer phases involved in the heterogeneous macromolecular alcohol reacting system were not mixed at the polymer chain level but remained segregated at a submicrometer scale (see TEM micrographs in Figure 5). Thus, at a first glance, large fractions of functional groups seemed to be excluded from collisions and reaction. This argument, together with the experimental fact that the overall reaction rate of the heterogeneous system was even much faster than the homogeneous analogous reacting system, suggests that the reaction rate in the interfacial regions be much higher than what would be expected from the homogeneous analogous reacting system. If this assumption is valid, one could then explain another experimental fact that the reaction kinetics of the homogeneous small alcohol systems was reaction controlled, whereas that of the heterogeneous macromolecular alcohol homologue was interfacial-area-generation controlled.

The validity of this assumption is seemingly supported by the dynamics of polymer chains at an interface. Consider an end-functionalized polymer chain whose reactive end is in an interface and main body in the bulk phase (Figure 9). Because of highly anisotropic friction with the neighboring chains, the relaxation (or snakelike motion) of the main body is a slow process, whereas that of the reactive end is a rapid one (Russell et al., 1993; Welp et al., 1999). As such, when two complementary functional groups are located within a "capture radius" (De Gennes, 1982a,b), the probability for them to collide is much higher than that for small molecule analogues because the much slower relaxation process of the main bodies holds

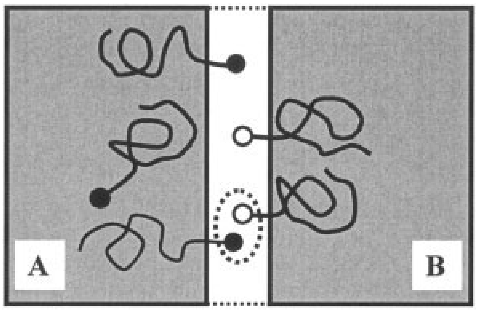

Figure 9. Reaction between complementary functional groups near or in an interface formed by two immiscible polymers A and B.

Of the two pairs of the complementary functional groups, one is located within a "capture radius" and another one is separated by a distance much greater than the capture radius.

them close to one another for a much longer period of time than small molecule counterparts. Relaxation of polymer chains depends very much on their molar masses. It will be much slower when full entanglement dynamics are operative. The latter require that the molar masses of the polymers be higher than 10 times their respective entanglement molar masses. The reactive polymers used in this work were about 3 times their entanglement molar masses, implying that the dynamics of our heterogeneous reacting system was likely somewhere between a Rouse regime and full-entanglement regime.

It should be noted that the above-mentioned collision probability increase is limited only to complementary functional groups that are located within the capture radius. Those located outside the capture radius, which are in very large quantities, will either "never" be able to approach one another to within the capture radius or need a very long time. This is why, without mixing, the reaction rate is virtually zero and why mixing is crucial. In addition to generating interfaces by the two mechanisms mentioned above, under certain circumstances mixing may cause relative displacement between the two phases of an interface–interfacial slip (Barsky and Robbins, 2002; Brochard-Wyart et al., 1990; Govas and Fredrickson, 1998; Zhao and Macosko, 2002), which allows complementary functional groups located outside the capture radius to approach each other and react. For a system composed of two immiscible polymers, the interfacial slip is related to the fact that the viscosity of the interfacial region (interfacial viscosity) can be much smaller than that of each of the two bulk polymers phases (bulk viscosity). This viscosity difference is attributed to the fact that chains located in the interfacial regions are much less entangled than in the bulk phases. However, it should be noted that the presence of a copolymer in the system, even in small amounts, can significantly reduce interfacial slip. This implies that the effect of interfacial slip may come into play only in the early stage of mixing where the copolymer areal density is low.

It is worthy noting that in a system composed of two immiscible polymers, there are more chain ends in the interface than in the bulk phases because of entropic adsorption (Reiter and Steiner, 1993; Zhao et al., 1993). If complementary functional groups like hydroxyl and isocyanate are attached to the chain ends, enrichment in functional groups in the interfaces is expected to be more important. This is because interactions between functional groups and polymer segments are often repulsive, and those between complementary functional groups are necessarily attractive. This enrichment also favors interfacial reactions.

In summary, this work showed that, under mixing, the reaction kinetics of immiscible reactive polymer systems significantly may exceed that of homogeneous small-molecule analogues. This was attributed to an increased collision frequency that resulted not only from mixing-induced interfacial area generation and interfacial copolymer pull-out, but also from slow relaxation process of reactive polymer chains, interfacial enrichment in functional groups, and eventually interfacial slip. This work also raised numerous issues worthy of further investigation. For example, only one pair of reactive polymers, PS and PMMA, was studied. The interfacial tension between them is relatively low ($\sim 2 \times 10^{-3}$ N/m) and the interfacial width quite large ($\sim$5 nm). The effects of interfacial tension and interfacial width should be critical on the interfacial reactions but were not addressed.

Conclusions

In this work, it has been shown that, contrary to common wisdom, for equivalent nominal molar concentrations in complementary functional groups, the overall reaction rate of those attached to two mutually immiscible polymer chains can exceed that of those attached to two mutually miscible small molecules, provided that mixing to which the reacting systems is subjected is strong enough. This result is attributed to an increased collision frequency that results not only from mixing-induced interfacial area generation and interfacial copolymer pull-out, but also from longer relaxation time of reactive polymer chains, interfacial enrichment in functional groups, and eventually interfacial slip. In addition to its scientific significance, the above result further explains why reactive polymer blending, a process of very short residence time (a dozen of seconds to a few minutes), has been so successful for producing polymer blends, an important family of polymer materials.

Acknowledgments

This work was supported by the Association Franco-Chinoise de la Recherche Scientifique et Technique (AFCRST) through PRA Mx02-07, the Embassy of the Republic of France in China through a scholarship to L.-F.F., and the National Natural Science Foundation of China (NSFC), Project 50290097.

Literature Cited

Baker, W., C. Scott, and G. H. Hu, *Reactive Polymer Blending*, Hanser, Munich, Germany (2001).

Ballard, D. G. H., G. D. Wignall, and J. Schelten, "Measurement of Molecular Dimensions of Polystyrene Chains in Bulk Polymer by Low-Angle Neutron Diffraction," *Eur. Polym. J.*, **9**, 965 (1973).

Barsky, S., and M. O. Robbins, "Molecular Dynamics Study of Slip at the Interface between Immiscible Polymers," *Phys. Rev. E*, **65**, 0.21801, 1 (2002).

Bhide, B.V., and J. J. Sudborough, "Esterification," *J. Indian Inst. Sci.*, **8A**, 89 (1925).

Brochard-Wyart, F., P. G. De Gennes, and S. Troian, "Slippage at the Interface between Two Slightly Incompatible Polymers," *Comptes rendus de l'Académie des Sciences, Série II: Chemistry*, **310**, 1169 (1990).

Charoensirisomboon, P., T. Inoue, and W. Weber, "Pull-Out of Copolymer In Situ–Formed during Reactive Blending: Effect of the Copolymer Architecture," *Polymer*, **41**, 6907 (2000).

De Gennes, P. G., "Kinetics of Diffusion-Controlled Processes in Dense Polymer Systems. I. Nonentangled Regimes," *J. Chem. Phys.*, **76**, 3316 (1982a).

De Gennes, P. G., "Kinetics of Diffusion-Controlled Processes in Dense Polymer Systems. II. Effects of Entanglements," *J. Chem. Phys.*, **76**, 3322 (1982b).

Flory, P. J., *Principle of Polymer Chemistry*, Cornell University Press, Ithaca, NY (1953).

Fredrickson, G. H., "Diffusion-Controlled Reactions at Polymer–Polymer Interfaces," *Phys. Rev. Lett.*, **76**, 3440 (1996).

Goveas, J. L., and Fredrickson, G. H. "Apparent Slip at a Polymer–Polymer Interface," *Eur. Phys. J. B: Condensed Matter Physics*, **2**, 79 (1998).

Guegan, P., C. W. Macosko, T. Ishizone, A. Hirao, and S. Nakahama, "Kinetics of Chain Coupling at Melt Interfaces," *Macromolecules*, **27**, 4993 (1994).

Hu, G. H., and Kadri, I. "Modeling Reactive Blending: An Experimental Approach," *J. Polym. Sci. Polym. Phys. Ed.*, **36**, 2153 (1998).

Hu, G. H., and Kadri, I., "Preparation of Macromolecular Tracers and Their Use for Studying the Residence Time Distribution of Polymeric Systems," *Polym. Eng. Sci.*, **39**, 299 (1999).

Hu, G. H., I. Kadri, and C. Picot, "On-line Measurement of the Residence

Time Distribution in Screw Extruders," *Polym. Eng. Sci.*, **39**, 930 (1999).

Li, H., "Formulation des mélanges de polymères dans un mélangeur interne: Développement d'un nouveau procédé d'élaboration d'un copolymère greffé et étude de ses rôles dans la formation de la stabilisation de la morphologie," Institut National Polytechnique de Lorraine, Nancy, France (2000).

Lyu, S.-P., J. J. Cernohous, F. Bates, and C. W. Macosko, "Interfacial Reaction Induced Roughening in Polymer Blends," *Macromolecules*, **32**, 106 (1999).

Mark, J. E., *Physical Properties of Polymers Handbook*, AIP, New York, p. 264 (1996).

Matsushita, Y., H. Momose, Y. Yoshida, and I. Noda, "Lamellar Domain Spacing of the ABB Graft Copolymers," *Polymer*, **38**, 149 (1997).

Odian, G., "*Principles of Polymerization,*" Wiley-Interscience, New York (1981).

O'Shaughnessy, B., and U. Sawhney, "Polymer Reaction Kinetics at Interfaces," *Phys. Rev. Lett.*, **76**, 3444 (1996).

Reiter, G., and U. Steiner, "Short-Time Dynamics of Polymer Diffusion across an Interface," *Prog. Colloid Polym. Sci.*, **91**, 93 (1993).

Rubinstein, M., and S. P. Obukhov, "Power-Law–Like Stress Relaxation of Block Copolymers: Disentanglement Regimes," *Macromolecules*, **26**, 1740 (1993).

Russell, T. P., V. R. Deline, W. D. Dozier, G. P. Felcher, G. Agrawal, R. P. Wool, and J. W. Mays, "Direct Observation of Reptation at Polymer Interfaces," *Nature*, **365**, 235 (1993).

Russell, T. P., A. Menelle, W. A. Hamilton, G. S. Smith, S. K. Satija, and C. F. Majkrzak, "Width of Homopolymer Interfaces in the Presence of Symmetric Diblock Copolymers," *Macromolecules*, **24**, 5721 (1991).

Semenov, A. N., "Theory of Microphase Layering in Block-Copolymer Melts," *Z. Eksp. 'noi i Teoretich. Fiziki*, **88**, 1242 (1985).

Ueberreiter, K., and M. Engel, "Investigations on the Kinetics of the Polycondensation of Sebacoyl Chloride with α,ω-Alkanediols," *Makromol. Chem.*, **178**, 2257 (1977).

Welp, K. A., R. P. Wool, G. Agrawal, S. K. Satija, S. Pispas, and J. Mays, "Direct Observation of Polymer Dynamics: Mobility Comparison between Central and End Section Chain Segments," *Macromolecules*, **32**, 5129 (1999).

Zhao, R., and C. W. Macosko, "Slip at Polymer–Polymer Interfaces: Rheological Measurements on Coextruded Multilayers," *J. Rheol.*, **46**, 145 (2002).

Zhao, W., X. Zhao, M. H. Rafailovich, J. Sokolov, R. J. Composto, S. D. Smith, T. P. Russell, W. D. Dozier, T. Mansfield, and M. Satkowski, "Segregation of Chain Ends to Polymer Melt Surfaces and Interfaces," *Macromolecules*, **26**, 561 (1993).

Appendix

Estimation of Σ

Consider a PS/PMMA reactive system in which the mass fractions of the PS, PS–$(CH_2)_2$–OH, the PMMA, and the PMMA-*r*-NCO are w, x, y, and z, respectively. The maximum amount of the in situ–formed graft copolymer is then $M(x + z)$, where M is the total mass of the reactive blend. If the PMMA particles are considered as spherical, then their number in the reactive blend is given by the following equation

$$n = \frac{\text{volume of the PMMA phase}}{\text{volume of a PMMA particule}} = \frac{M(y+z)/\rho_{\mathrm{PMMA}}}{\pi d^3/6} \qquad (1\mathrm{A})$$

where d and ρ_{PMMA} are the diameter and the volumetric mass of PMMA, respectively.

If all copolymer chains are located at the interfaces, then Σ is given by

$$\Sigma = \frac{\text{number of copolymer chains}}{\text{total surface area of the PMMA phase}} = \frac{M(x+z)pN_A/\bar{M}_n}{\pi d^2 n} \qquad (2\mathrm{A})$$

where $\bar{M}_n$ is the number-average molar mass of the graft copolymer, N_A is Avogadro's number, and p is thethe fraction of the maximum amount of copolymer attainable. From Eqs. A1 and A2, one obtains

$$\Sigma = \frac{1}{6}\frac{x+z}{y+z}\frac{\rho_{\mathrm{PMMA}}N_A}{\bar{M}_n}dp \qquad (3\mathrm{A})$$

All the parameters involved in the above equation are known except for ρ_{PMMA} and $\bar{M}_n$. The latter was between 81.6 (the inversed Y-shaped graft copolymer with one PS graft) and 109.5 kg/mol (the inversed Π-shaped graft copolymer with two PS grafts). For the sake of rough estimation over Σ, it was taken as 95.6 kg/mol, the average value of the above two. ρ_{PMMA} at 175°C was taken as 1 g/cm^3.

Estimation of Σ_{max}

Consider a plane interface covered by a dense monolayer of an immiscible A–B block copolymer, denoted as A-*b*-B. The thickness of the monolayer should be about half of the lamellar spacing, $\lambda_{\text{A-}b\text{-B}}/2$, in the ordered bulk block copolymer. Thus, Σ_{max} can be estimated using the following equation

$$\Sigma_{max} = \frac{\text{half of the lamellar spacing}}{\text{volume of a copolymer chain}} = \frac{\lambda_{\text{A-}b\text{-B}}/2}{\bar{M}_n/(N_A\rho_{\text{A-}b\text{-B}})} = \frac{1}{2}\frac{\lambda_{\text{A-}b\text{-B}}N_A\rho_{\text{A-}b\text{-B}}}{\bar{M}_n} \qquad (4\mathrm{A})$$

The dependency of the micelle spacing on the properties of a diblock such as molar mass, segment length, and interaction parameter is well understood in terms of mean field theory in the strong segregation limit. Their lamellar spacing $\lambda_{\text{A-}b\text{-B}}$ is given by Semenov (1985) and Rubinstein and Obukhov (1993)

$$\lambda_{\text{A-}b\text{-B}} = 1.10aN^{1/2}(\chi N)^{1/6} \qquad (5\mathrm{A})$$

where a is the statistical segment length, N is the total number of monomers in the diblock, and χ is the interaction parameter between the two component polymers. The derivation assumes that the latter have similar statistical segment lengths, which is the case for PS and PMMA. The value of the statistical segment length for PS is 0.68 nm and that for PMMA is 0.69 nm (Ballard et al., 1973). However, the assumption of the strong segregation limit may not be met, considering the relatively low interaction parameter between them. Because of this, we assume that the scaling law of Eq. A5 remains valid, that is

$$\lambda_{\text{A-}b\text{-B}} = kN^{2/3} \qquad (6\mathrm{A})$$

The lamellar spacing of a Y-shaped immiscible A-*b*-B graft copolymer with A as the trunk chain, $\lambda_{\text{A-}g\text{-B}}$, can be related to that of the corresponding A-*b*-B block copolymer by the following equation (Matsushita et al., 1997):

$$\lambda_{\text{A-}g\text{-B}} = (4 - 3\phi_B)^{-1/3}\lambda_{\text{A-}b\text{-B}} \tag{7A}$$

The lamellar spacing of a block copolymer of styrene and methyl methacrylate having a value of $\bar{M}_n = 100.9$ kg/mol (52.9 and 48.0 kg/mol for the PS and PMMA blocks, respectively) was found to be 39.8 nm (Russell et al., 1991). If $\rho_{\text{PS-}g\text{-PMMA}}$ is taken as 1 g/cm^3 and ϕ_{PS} as 0.42 (the average of the composition of the graft copolymer with one PS graft and that of the graft copolymer with two PS grafts), the use of Eqs. A4–A7 yields $\Sigma_{max} = 0.085$ chain/nm^2. Considering the numerous crude approximations involved, the real value of Σ_{max} could be somewhere between 0.07 and 0.10 chain/nm^2.

Manuscript received Jul. 28, 2003, and revision received Jan. 21, 2004.